Environment Protection Engineering

Vol. 43 2017 No. 3

DOI: 10.5277/epe170311

ULKER ASLI GULER[1], MELTEM SARIOGLU CEBECI[1]

POTENTIAL OF PUMICE MODIFIED WITH IRON(III) FOR COPPER REMOVAL FROM AQUEOUS SOLUTIONS

Iron-modified pumice (Fe-P) was prepared by the ion-exchange method using natural pumice from Kayseri, Turkey at room temperature without calcination. SEM, FTIR, XRD, and S_{BET} measurement were used to investigate the copper removal mechanism. The results show that the S_{BET} of the pumice increased from 11.88 m^2/g to 21.01 m^2/g after iron modification. The effects of pH, contact time, initial copper concentration, temperature, and various cations (Na^+, K^+, Ca^{2+}, Mg^{2+} and Al^{3+}) at various pH were investigated in batch experiments. More than 92% of Cu(II) was removed after 180 min. Langmuir, Freundlich, Dubinin–Radushkevich and Temkin isotherm models were applied to the equilibrium data at 298, 308 and 318 K. The maximum adsorption capacity at 298, 308 and 318 K was found to be 21.52, 19.48, and 19.67 mg/g, respectively. The kinetics of copper on Fe-P was best described by the pseudo-second order kinetic model. The negative values of free energy change and enthalpy change indicated that the adsorption process was feasible, spontaneous and exothermic.

1. INTRODUCTION

Many industrial wastewaters such as metal working, mining, steel, electric and electronic manufacturing, electroplating, refining process, batteries and the paint industry are contaminated with heavy metals [1–3]. Treatment of these industrial wastewaters is very important because of their high toxicity to humans, animals, and plants. Requirements for complying with environmental legislation are becoming increasingly more stringent [4]. The removal of heavy metal ions from aqueous solutions has been commonly carried out by processes such as oxidation, chemical precipitation, ion exchange, adsorption, biosorption, membrane filtration, reverse osmosis, and biological methods [5, 6]. Adsorption is effective for removing heavy metals from dilute solutions and is commonly used because the adsorbent is reusable, has a low operating cost and short operating times, can target specific metals, and does not generate toxic by-products [7, 8].

[1]Cumhuriyet University, Environmental Engineering Department of Engineering Faculty, Sivas, Turkey, 58140, corresponding author U.A. Guler, e-mail address: ulkerasli@gmail.com

Nowadays, many researchers have focused on inexpensive materials such as kaolinite, lignite, fly ash, sawdust, plant wastes, and biomass for the removal of heavy metals from wastewaters [5–10].

Pumice is a volcanic stone with higher surface area and porosity. Natural and modified pumice have been recently used as adsorbent, filter beds, and support material in water and wastewater treatment [11].

The aim of the present study was to investigate the possibility of Cu(II) adsorption onto iron-modified pumice (Fe-P). It was characterized by SEM, FTIR, XRD and specific surface area (S_{BET}) determination in order to discuss the adsorption mechanism. pH, contact time, initial copper concentration, temperature, and effeccts of various cations (Na^+, K^+, Ca^{2+}, Mg^{2+} and Al^{3+}) at various pH were investigated, as well as the equilibrium, kinetics and thermodynamics of the adsorption process.

2. EXPERIMENTAL

Materials and chemicals. Pumice was obtained from Kayseri-Basakpınar in Turkey. Its chemical composition was as follows: SiO_2 69.27 wt. %, Al_2O_3 22.1 wt. %, K_2O 3.89 wt. %, Na_2O 3.61 wt. %, Fe_2O_3 2.90 wt. %, CaO 1.82 wt. % and small amounts of Mg, Ti, S, P, Mn, Ba, Zr, Cr and Zn. It was washed with distilled water several times and dried in an oven at 50 °C. Later, particle size of dried pumice was round to less than 0.125 mm. All chemicals were of analytical grade purity. Copper was used as the adsorbate. A stock copper solution (1000 mg/dm^3) was initially prepared by dissolving $CuSO_4 \cdot 5H_2O$ in distilled water and preserved with concentrated HNO_3.

Modification of pumice with iron. Samples of Fe-P were prepared using Fe(III) by the ion-exchange method [12]. First, pumice was pretreated in a 37 wt. % solution of HCl for 24 h at room temperature under mechanical stirring at 130 rpm. Samples were washed 2–3 times with distilled water and oven-dried at 103 °C. The pretreated pumice was then placed in a glass beaker and a solution of 0.5 M Fe(III) was added under agitation until all pretreated pumice was soaked in the solution. Next, a 3 M NaOH solution was added while mixing until pH reached ca. 9.5, and then constant stirring continued for 30 min. Subsequently, the mixture was dried at 50 °C for 50 h while mixing and then dried in an oven at 50 °C for about 50 h. The prepared material was washed with distilled water to remove granular iron oxide particles and then dried at 80 °C for 24 h and 50 °C for about 48 h. The prepared Fe-P was stored in brown bottles for later use. As an indicator of a successful coating, a yellow-brown color change occurred in the pumice after being coated in iron.

Batch experiments. For the batch experiments 100 cm^3 samples of Cu(II) solution in 250 cm^3 Erlenmeyer flasks were used. Effects of pH (2–6), contact time (2–1440 min), initial Cu(II) concentration (10–250 mg/dm^3), temperature (25–45 °C) on adsorption were

investigated by varying one parameter at a time and keeping the remaining other parameters constant. The effect of various cations was investigated by adjusting pH from 6 to 2 with HCl and NaOH solutions and keeping initial concentration of Cu(II) constant at 50 mg/dm^3. The experimental conditions are presented in Table 1. Optimum pH was selected by favoring the adsorption of Cu(II), which was then used in subsequent kinetic, isotherm and thermodynamic experiments. The residual concentration of Cu(II) in the supernatant was analyzed using a Nova 60 UV spectrophotometer.

Table 1

Experimental conditions

Set	Experimental aim Effect of a factor	pH	$[Cu(II)]_0$ [mg/dm^3]	Adsorbent dose [g/dm^3]	Contact time [min]	Temperature [°C]
1	pH	2–6	50	5	1440	25
2	Contact time	5	50	5	2–1440	25
3	Initial Cu(II) concentration	5	10–250	5	180	25–45
4	Cations (Na^+, K^+, Ca^{2+}, Mg^{2+}, Al^{3+})	2–6	50	5	180	25
7	Temperature	5	50	5	180	25–45

Cu(II) removal efficiency (*RE*, %) and adsorption capacity (q_e, mg/g) were calculated with the following equations (1,2):

$$RE = \frac{C_0 - C_e}{C_0} \times 100\% \tag{1}$$

$$q_e = \frac{(C_0 - C_e)V}{m} \tag{2}$$

where C_0 and C_e are the initial and the equilibrium Cu(II) concentration (mg/dm^3), V is the volume of solution (dm^3) and m is the weight of Fe-P (g).

Characterization methods. The morphological analysis of Fe-P was performed using SEM, FTIR and XRD analyses. The S_{BET} of natural pumice and Fe-P was measured by the Brunauer–Emmett–Teller (BET) N_2 method.

The point of zero charge (pzc). 100 cm^3 of 0.1 M KCl solution was placed in an Erlenmeyer flask and the initial pH was adjusted from 1 to 12 with H_2SO_4 or NaOH solution. Then 0.5 g natural pumice or Fe-P was added to the solution. The mixtures were shaken for 24 h to reach equilibrium. The final pH vs. initial pH was plotted. At pH_{pzc} ($\Delta pH = pH_{final} - pH_{initial} = 0$) [13, 14].

Adsorption kinetics. Pseudo-first order, pseudo-second order and intraparticle diffusion models were used. Non-linear pseudo-first and pseudo-second order kinetic models are described by the following equations [15, 16]:

- pseudo-first order model

$$q_t = q_e(1 - e^{-k_1 t}) \tag{3}$$

- pseudo-second order model

$$q_t = \frac{k_2 q_e^2 t}{1 + k_2 q_e t} \tag{4}$$

where q_e and q_t are the amounts of adsorbed Cu(II) on adsorbent at equilibrium and time t (mg/g), k_1 (min^{-1}) and k_2 (g/(mg·min)) are the rate constants of pseudo-first and pseudo--second order processes, respectively.

Intraparticle model is expressed as [17]:

$$q_t = k_i t^{0.5} + C \tag{5}$$

where k_i (mg/(g·$min^{0.5}$)) and C are the rate constant of intraparticle diffusion model and the intercept, respectively.

Equilibrium studies. The adsorption isotherm of Cu(II) was determined at 298, 208 and 318 K. The Langmuir, Freundlich, Dubinin–Radushkevich (D–R) and Temkin isotherm model were used to fit the experimental data [18, 19].

The Langmuir isotherm is a single layer adsorption model which can be expressed as:

$$q_e = \frac{Q_m b C_e}{1 + b C_e} \tag{6}$$

where, Q_m is the maximum adsorption capacity (mg/g) and b is the Langmuir constant (dm^3/mg).

The Freundlich isotherm for heterogeneous surfaces is expressed by

$$q_e = k_F C_e^{1/n} \tag{7}$$

where, k_F is the Freundlich adsorption constant (dm^3/g) and n is the adsorption intensity.

To distinguish between the physical and chemical sorption onto Fe-P, D–R isotherm based on the heterogeneous nature of the sorbent surface is applied. The D–R isotherm equation is given as equation (8).

$$q_e = q_{D-R} e^{\beta \varepsilon^2} \tag{8}$$

where $q_{D–R}$ is the maximum adsorption capacity (mol/g), β is a coefficient related to the mean free energy of adsorption (mol^2/J^2), and ε is the Polanyi potential (J/mol)

$$\varepsilon = RT \ln\left(1 + \frac{1}{C_e}\right)$$

The mean free energy E (kJ/mol) is then derived from:

$$E = \frac{1}{\sqrt{-2\beta}} \tag{9}$$

The Temkin isotherm has been developed taking into account the interaction between an adsorbent and adsorbed agents. It is expressed by the following equation

$$q_e = \frac{RT}{b_T} \ln\left(K_T C_e\right) \tag{10}$$

where b_T is a constant (g·kJ/(mg·mol)), and K_T – an equilibrium binding constant (dm^3/mg).

Thermodynamic studies. The thermodynamic parameters such as changes of Gibbs free energy *(*$\Delta G°$*)*, enthalpy ($\Delta H°$), and entropy ($\Delta S°$) were used to evaluate the spontaneity, nature of the process and randomness at the adsorbent–adsorbate interface. The following equations were used [20]:

$$\ln K_c = \frac{\Delta S°}{R} - \frac{\Delta H°}{RT} \tag{11}$$

$$\Delta G° = -RT \ln K_c \tag{12}$$

where, K_c (q_e/C_e) is the equilibrium constant. The values of $\Delta H°$ and $\Delta S°$ were determined from a slope and intercept of the linear plot of lnK_c vs. 1/T, respectively.

3. RESULTS AND DISCUSSION

3.1. CHARACTERIZATION OF THE MATERIAL

The properties of pumice and Fe-P are given in Table 2. The S_{BET}, total pore volume, and average pore diameter of pumice and Fe-P were 11.88 m^2·g^{-1}, 0.041 cm^3·g^{-1}, 13.81 nm

and 21.01 $m^2 \cdot g^{-1}$, 0.041 $cm^3 \cdot g^{-1}$, 7.82 nm, respectively. The values of S_{BET} and average pore diameter changed as a result of iron coating. S_{BET} of modified pumice increased while average pore diameter of modified pumice decreased.

Table 2

Characteristics of natural and modified (Fe-P) pumice

Material	S_{BET} [m^2/g]	Total pore volume [cm^3/g]	Average pore diameter [nm]	pH_{pzc}
Pumice	11.88	0.041	13.81	8.34
Fe-P	21.01	0.041	7.82	7.59

XRD spectra of pumice, Fe-P before, and Fe-P after Cu(II) removal (Fe-P-Cu) are presented in Fig. 1. In the XRD analyses, three peaks were observed for pumice at 22°, 28°, 59° and for Fe-P at 24°, 28°, and 42°, respectively. This finding reveals an amorphous quartz substance [11]. In addition, the apparent peak at 42° in Fe-P indicated the presence of iron, which was supported on the pumice surface [21, 22]. The peak at 28° of Fe-P-Cu is very clear. The changes of peaks are an evidence of Cu(II) adsorption.

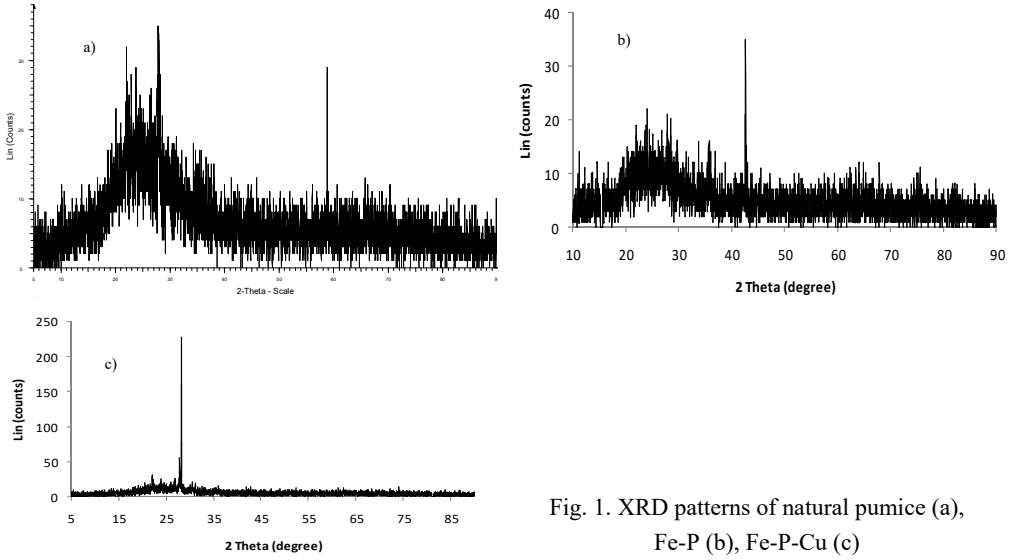

Fig. 1. XRD patterns of natural pumice (a), Fe-P (b), Fe-P-Cu (c)

The FTIR spectrum of pumice, Fe-P and Fe-P-Cu are presented in Fig. 2. Characteristic peaks of pumice are 800 cm–1, 1700 cm–1, 2300 cm–1 and 3500 cm–1. The peaks at 800 $cm^{-1}$and 1700 cm^{-1} may correspond to Si–O bending vibrations of the amorphous quartz and be assigned to amide I or C=O amide stretching, respectively [11]. Peaks of Fe-P at 2328 cm^{-1}, and 1042 cm^{-1} disappeared. The peaks of Fe-P-Cu appeared at 3233 cm^{-1},

1635 cm^{-1}, 1008 cm^{-1} and 780 cm^{-1}. A broad band around 3233 cm^{-1} of Fe-P-Cu corresponds to vibrations of –OH groups [23].

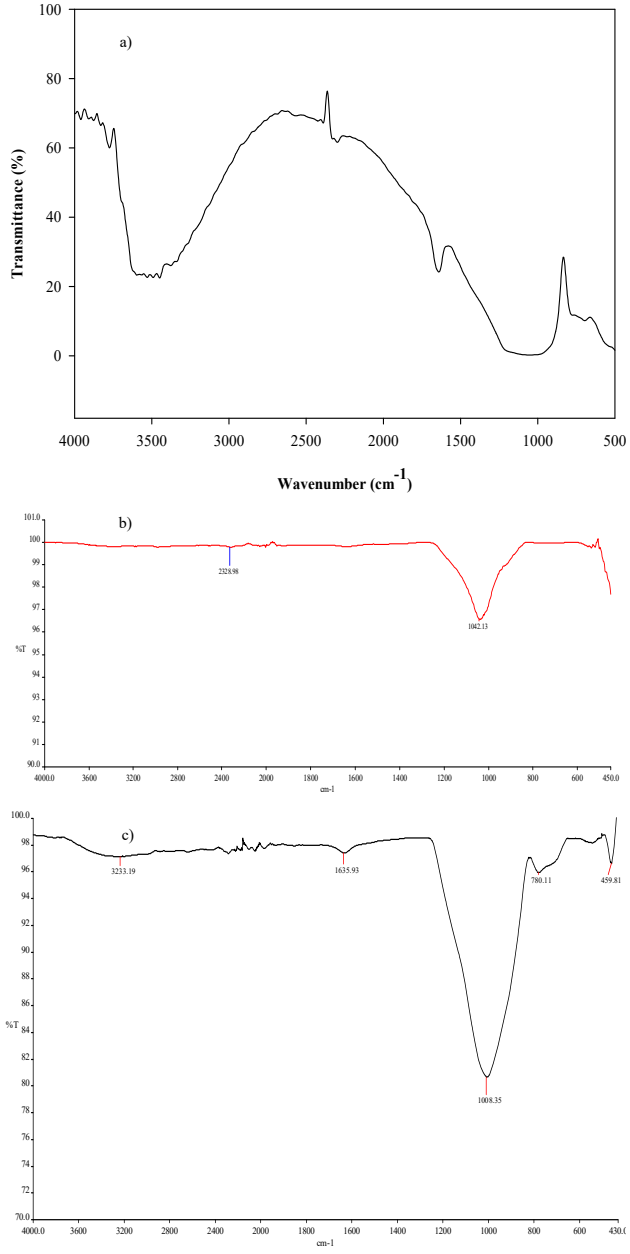

Fig. 2. FTIR spectra of natural pumice (a), Fe-P (b), and Fe-P-Cu (c)

The peak at 1635 cm^{-1} of Fe-P-Cu shows changes in the amide I or C=O amide groups [24]. The reason of this is cation exchange and surface adsorption with surface complexation. In addition, the peak observed at 780 cm^{-1} in Fe-P-Cu represents Si–O structure [11]. Characteristic stretching vibrations for Si–O–Si bands were observed at 1042 and 1008 cm^{-1} [23, 25].

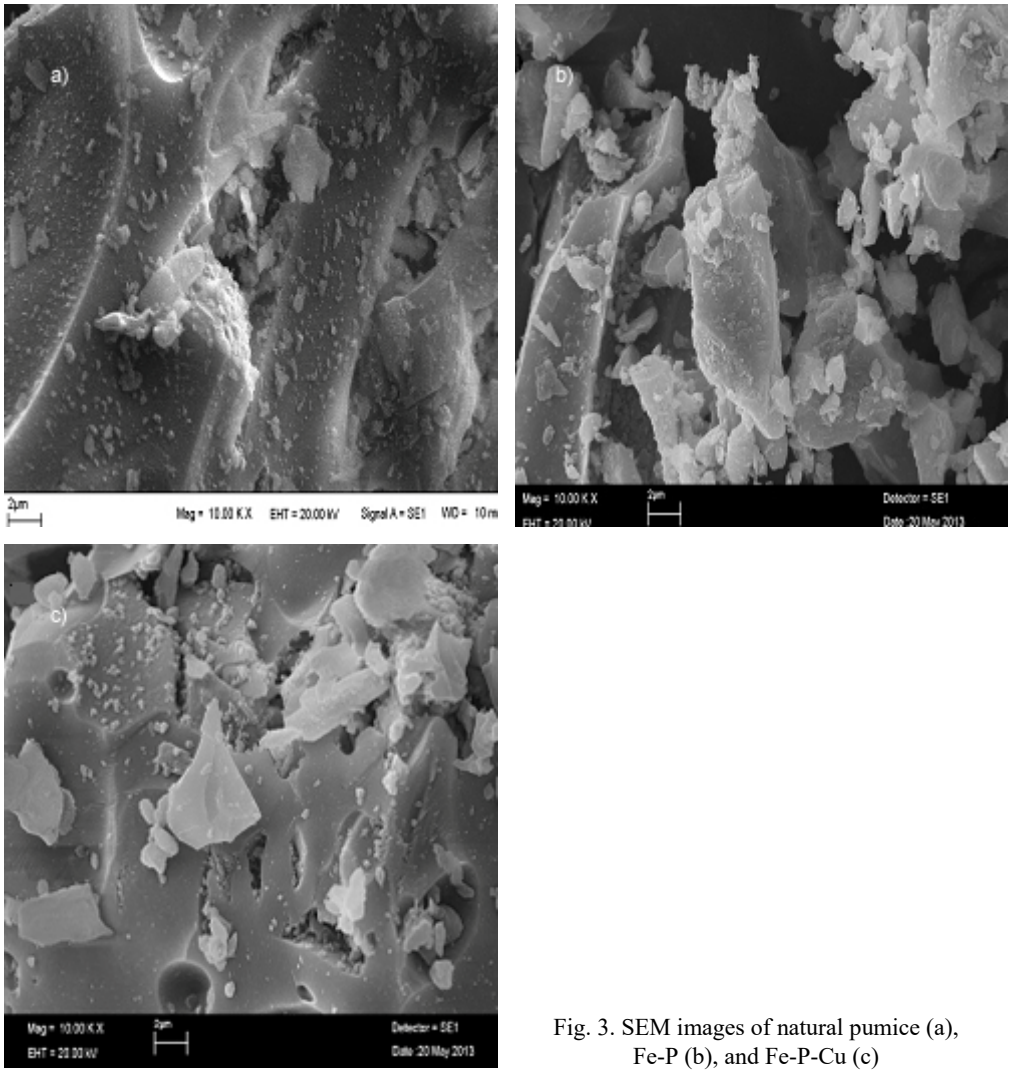

Fig. 3. SEM images of natural pumice (a), Fe-P (b), and Fe-P-Cu (c)

SEM images of pumice, Fe-P, and Fe-P-Cu are presented in Fig. 3. Pumice has a smooth, even, and porous structure. Differentiated and porous channels and spaces cannot be seen clearly from the SEM images after iron modification. The reason for this

is the coating of the outer surface with iron oxides. (cf. [23, 26]). The SEM image of Fe-P-Cu showed that the surface and cavities were filled with Cu(II) ions.

3.2. EFFECT OF pH

pH of the solution has an important role in adsorption. It affects the ionization of functional groups and the competitiveness of ions in solution. Studies were carried out to see the effect of pH, in the range of 2–6. In the study, initial Cu(II) concentration was fixed at 50 mg/dm^3, and the adsorbent dose was 5 g/dm^3. The effect of pH on the Cu(II) removal and determination of pH_{pzc} are presented in Fig. 4.

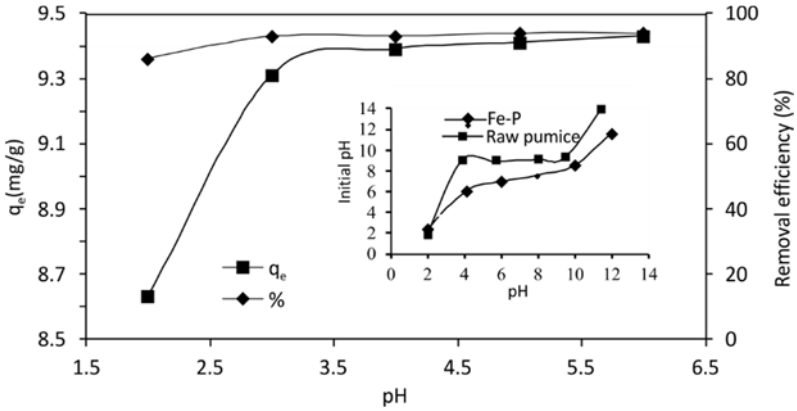

Fig. 4. Effect of pH on the Cu(II) removal efficiency and adsorption capacity of modified pumice (Fe-P); C_0 50 mg/dm^3, adsorbent dose 5 g/dm^3, contact time 1440 min, 25 °C

The removal of Cu(II) increased from 86% to 94% upon increasing pH. Cu(II) removal efficiency and adsorption capacity of Fe-P at pH 5 and 6 reached 94%, 9.41 mg/g and 94%, 9.43 mg/g, respectively. The decrease in Cu(II) removal under acidic conditions may be due to the competition of excess of hydrogen ions with Cu(II) ions for active sites on Fe-P. The pH_{pzc} of raw pumice and Fe-P were found to be around 8.34 and 7.59, respectively; this indicates that the surface of Fe-P is positively charged at pH <7.59 and negatively charged for its lower values [13]. In the adsorption process, Cu(II) ions replaced protons on the Fe-P surface, which was confirmed by the fact that protons were released into the solution during adsorption [14]. In the literature, pH_{pzc} values of pumice and iron oxides are 6.9–9.3 and 6–9, respectively [27]. Iron coating increased the amount of total surface acidic groups of the material and the value of pH_{pzc} decreased [28]. The modification of pumice by iron oxide affected pore structures and surface areas as well as the surface chemistry of pumice. The maximal removal of Cu(II) was achieved at pH 5 and 6, respectively. The experiments were performed at pH 5.

3.3. EFFECT OF CONTACT TIME AND KINETIC MODELING

The effect of contact time on the removal of Cu(II) onto Fe-P is shown in Fig. 5. Cu(II) adsorption onto Fe-P occurred in sequential equilibrium steps. Adsorption was completed in 72% after 30 min and later it slowly reached equilibrium. At the end of 180 min, removal efficiency and adsorption capacity reached 92% and 9.17 mg/g, respectively.

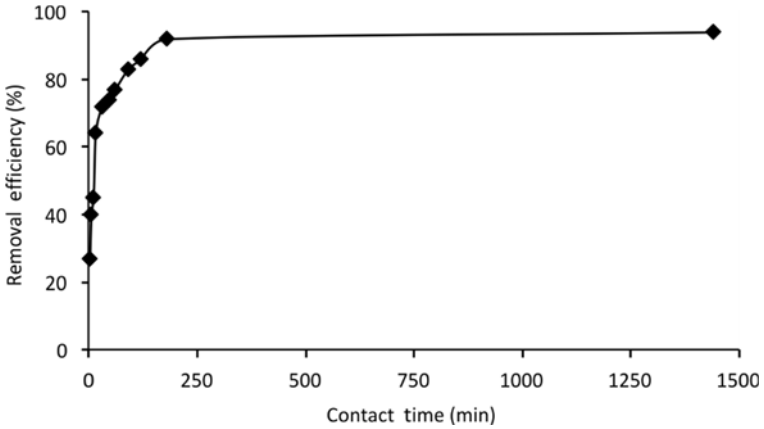

Fig. 5. Effect of contact time on the Cu(II) removal efficiency by adsorption on modified pumice (Fe-P)
C_0 50 mg/dm^3, adsorbent dose 5 g/dm^3, contact time 1440 min, 25 °C

The calculated coefficients and correlation coefficients (R^2) are listed in Table 3.

Table 3

Kinetic parameters of the Cu(II) adsorption

	Pseudo-first order			Pseudo-second order			Intra particle diffusion		
q_e [mg/g]	k_1 [min^{-1}]	q_1 [mg/g]	R^2	k_2 [g/(mg·min)]	q_2 [mg/g]	R^2	k_i [mg/(g·min)$^{0.5}$]	C	R^2
9.17 mg/g	0.018	4.86	0.921	0.0099	9.34	0.996	0.587	2.995	0.863

Cu(II) adsorption fitted well to a pseudo-second-order kinetic model (R^2 = 0.996). The q_2 values are very close to those calculated. This indicates that there is a chemical process which is a rate limiting step in which ion exchange between Fe-P and Cu(II) ions or a complex formation and adsorption depends on pollutant concentration [15, 29, 30]. According to the intraparticle diffusion model, in the adsorption process both boundary layer diffusion and intraparticle diffusion ($C \neq 0$) occur [18].

3.4. EFFECT OF INITIAL Cu(II) CONCENTRATION AT VARIOUS TEMPERATURES

The initial concentration of the contaminant provides an important driving force against the mass transfer resistance of all molecules between the sorbent and sorbate [18]. This study evaluated Cu(II) concentrations from 10–250 mg/dm^3 at 25–45 °C (Fig. 6).

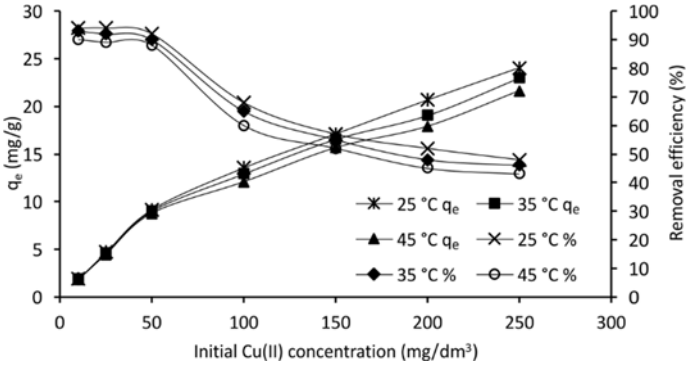

Fig. 6. Effect of initial Cu(II) concentration on the removal efficiency and adsorption capacity of modified pumice (Fe-P); pH 5, adsorbent dose 5 g/dm^3, contact time 180 min

The adsorption capacity increased upon increasing initial Cu(II) concentration and removal efficiency decreased. This can be explained by increased interaction between Cu(II) and Fe-P due to higher concentrations of Cu(II) [18]. Decrease of the adsorption capacity upon increasing temperature is due to the exothermic nature of the removal process.

Cu(II) removal on a natural pumice was also studied (C_0 = 50 mg/dm^3, contact time 180 min, pH 5, 25 °C, and 5 g/dm^3 of the adsorbent). The 63% removal efficiency with natural pumice was achieved while 92% removal on Fe-P was provided. These results showed that the modification with iron substantially increased the removal efficiency for Cu(II).

3.5. EFFECT OF VARIOUS CATIONS

The effect of various cations such as Na^+, Al^{3+}, K^+, Ca^{2+}, Mg^{2+} on Cu(II) removal was studied at various pH (Fig. 7). Adsorption capacity of Cu(II) was only affected by K^+ and not by other cations. The effects of divalent cations were different from monovalent cations. Cu(II) may form strong inner-sphere complexes with Fe-P surface. Na^+, K^+, Ca^{2+} and Mg^{2+} may form weakly outer-sphere complexes and they could hardly influence strong inner-sphere complexes between Cu(II) and Fe-P [31]. Therefore, Cu(II) adsorption was not dependent on ionic strength.

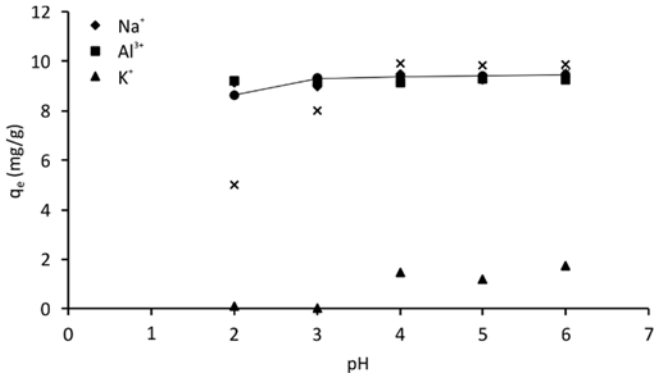

Fig. 7. Effect of various cations on the adsorption capacity of modified pumice (Fe-P) towards Cu(II); C_0 50 mg/dm^3, adsorbent dose 5 g/dm^3, pH 5, 25 °C, cation concentration 0.01 M

3.6. ADSORPTION ISOTHERMS

Langmuir, Freundlich, Dubinin–Radushkevich (D–R), and Temkin isotherm models were applied to the equilibrium data. The isotherms are presented in Fig. 8 and isotherm model constants and correlation coefficients (R^2) are presented in Table 4.

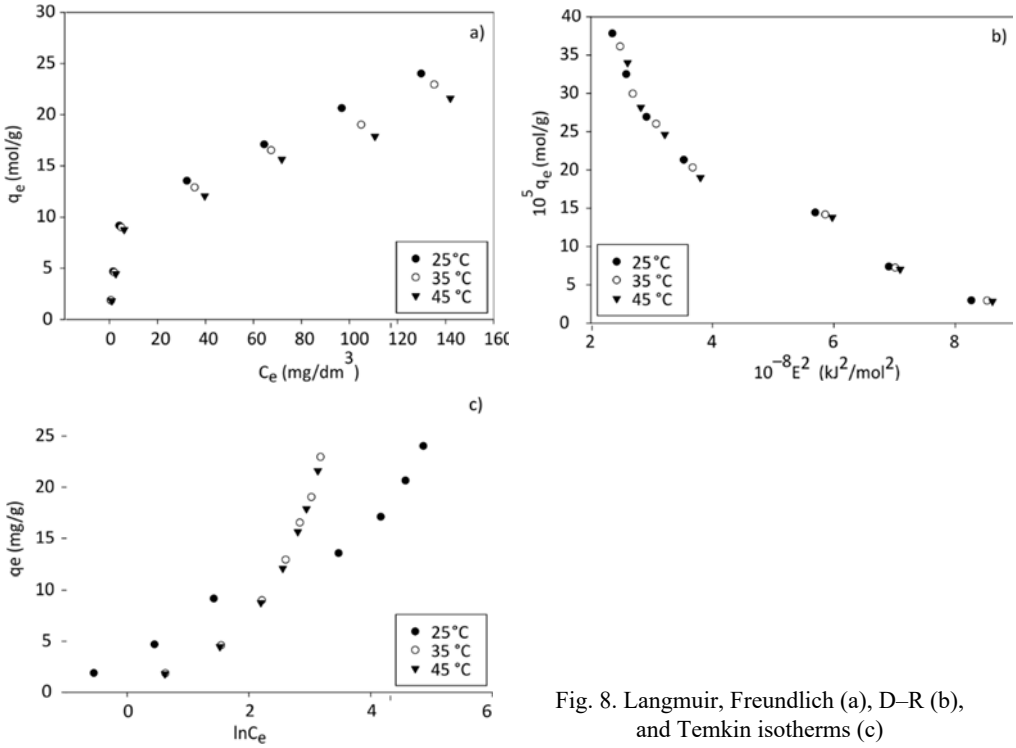

Fig. 8. Langmuir, Freundlich (a), D–R (b), and Temkin isotherms (c)

R^2 values in the Freundlich isotherm model are higher than in the Langmuir model. This demonstrates that the Cu(II) adsorption occurred on heterogenic surfaces. The maximum adsorption capacity (Q_m) decreased as temperature increased It was 21.52 mg/g at 25 °C, 19.48 mg/g at 35 °C, and 19.67 mg/g at 45 °C. Also, 1/n values were between 0 and 1, indicating that adsorption was favorable at these conditions.

As shown in Table 4, R^2 values in the D–R isotherm model are quite high (0.98). The average adsorption energy (E) is between 8 and 16 kJ/mol for all three temperatures. When E is between 8–16 kJ/mol, it means that an adsorption mainly takes place via ion exchange mechanism, which is a chemical process. If E is lower than 8 kJ/mol, the adsorption mechanism can be explained by physical interactions [19]. According to the Temkin isotherm model, as the surface is coated, the adsorption heat of all molecules on the surface for Cu(II) decreases linearly due to the interactions between adsorbent and adsorbate.

Table 4

Langmuir, Freundlich, D–R and Temkin adsorption isotherm parameters for Cu(II) adsorption onto Fe-P

Temperature [°C]	Langmuir			Freundlich			
	Q_m [mg/g]	b [dm^3/mg]	R^2	k_F [dm^3/g]	n	R^2	
25	21.52	0.129	0.953	4.11	2.81	0.988	
35	19.48	0.118	0.954	3.75	2.79	0.986	
45	19.67	0.091	0.954	3.28	2.70	0.984	
	Temkin			D–R			
	b_T [g·kJ/(mg·mol)]	K_T [dm^3/mg]	R^2	$q_{D–R}$ [mol/g]	E [J/mol]	10^9B [mol^2/J^2]	R^2
25	668	2.4	0.978	8×10^{-4}	11.94	3.51^9	0.985
35	321	4.8	0.949	8×10^{-4}	12.19	3.37	0.984
45	347	4.9	0.950	7×10^{-4}	12.29	3.31	0.982

3.7. THERMODYNAMIC STUDIES

The effect of temperature on Cu(II) adsorption was studied at three temperatures (Fig. 6). This parameter could be important for energy-dependent mechanisms in Cu(II) adsorption by Fe-P [32]. The coefficients of the thermodynamic model and correlation constants (R^2) are presented in Table 5.

Negative values of $\Delta H°$ indicate the Cu(II) adsorption was exothermic. In environmental engineering applications, both energy and entropy parameters must be considered in order to examine which process may occur spontaneously [32]. The Gibbs free energy change, $\Delta G°$, is spontaneous and feasible. A positive value of $\Delta S°$ showed that the adsorption process increased in randomness at the solid–liquid interface during adsorption.

Table 5

Thermodynamic functions

Function	$\Delta H°$ [kJ/mol]	$\Delta S°$ [kJ/(mol·K)]	$\Delta G°$ [kJ/mol]		
			298	308	318
Value	–17.87	3.28	–19.07	–19.20	–19.22

4. CONCLUSIONS

The adsorption capacity of iron-modified pumice towards Cu(II) was studied in various experimental conditions. When compared with the natural pumice, iron-modified pumice had a much larger specific surface area as a result of the functionalization of the mesoporous pumice with iron. The modified pumice showed great affinity towards Cu(II). In the adsorption process, equilibrium data are described by a Freundlich isotherm model. The maximum adsorption capacity (Q_m) obtained from a Langmuir isotherm model decreased upon increasing temperature (21.52 mg/g at 25 °C, 19.48 mg/g at 35 °C, and 19.67 mg/g at 45 °C). During first 30 min of contact time, iron-modified pumice removed the Cu(II) ions rapidly due via active surface sites. The adsorption process of Cu(II) on Fe-P was exothermic and spontaneous. According to the kinetic tests, a pseudo-second order model best fits the adsorption data. The mechanism of Cu(II) adsorption is probably due to a combination of cation exchange and surface complexation.

ACKNOWLEDGMENTS

The authors thank the Research and Application Center of Erciyes University (TAUM), for their help in XRD, FTIR and SEM analyses.

REFERENCES

[1] AGUADO J., ARSUAGA J.M., ARENCIBIA A., LINDO M., GASCON V., *Aqueous heavy metals removal by adsorption on amine-functionalized mesoporous silica*, J. Hazard. Mater., 2009, 163, 213.

[2] RAO M.M., RAMESH A., RAO G.P.C., SESHAIAH K., *Removal of copper and cadmium from the aqueous solutions by activated carbon derived from Ceiba pentandra hulls*, J. Hazard. Mater., 2006, 129, 123.

[3] MILICEVIC S., BOLJANAC T., MARTINOVIC S., VLAHOVIC M., MILOSEVIC V., BABIC B., *Removal of copper from aqueous solutions by low cost adsorbent – Kolubara lignite*, Fuel Proc. Techn., 2012, 95 (1), 7.

[4] AL-RASHDI B., TIZAOUI C., HILAL N., *Copper removal from aqueous solutions using nano-scale diboron trioxide/titanium dioxide (B_2O_3/TiO_2) adsorbent*, Chem. Eng. J., 2012, 183, 294.

[5] PAPANDREOU A., STOURNARS C.J., PANIAS D., *Copper and cadmium adsorption on pellets made from fired coal fly ash*, J. Hazard. Mater., 2007, 148, 538.

[6] PENTARI D., PERDIKATSIS V., KATSHIMICHA D., KANAKI A., *Sorption properties of low calorific value Greek lignites. Removal of lead, cadmium, zinc and copper ions from aqueous solutions*, J. Hazard. Mater., 2009, 168, 1017.

[7] KILIC M., YAZICI H., SOLAK M., *A comprehensive study on removal and recovery of copper(II) from aqueous solutions by NaOH-pretreated Marrubium globosum ssp., globosum leaves powder. Potential for utilizing the copper(II) condensed desorption solutions in agricultural applications*, Bioresour. Technol., 2009, 100, 2130.

[8] XIA L., HU Y.X., ZHANG B.H., *Kinetics and equilibrium adsorption of copper(II) and nickel(II) ions from aqueous solution using sawdust xanthate modified with ethanediamine*, Trans. Nonferrous Met. Soc. China, 2014, 24, 868.

[9] WAN NGAH W.S., HANAFIAH M.A.K.M., *Removal of heavy metal ions from wastewater by chemically modified plant wastes as adsorbents. A review*, Bioresour. Technol., 2008, 99 (10), 3935.

[10] ZHANG X., LIN S., CHEN Z., MEGHARAJ M., NAIDU R., *Kaolinite-supported nanoscale zero-valent iron for removal of Pb^{2+} from aqueous solution. Reactivity, characterization and mechanism*, Water Res., 2011, 45, 3481.

[11] GULER U.A., SARIOGLU M., *Removal of tetracycline from wastewater using pumice stone. Equilibrium, kinetic and thermodynamic studies*, J. Environ. Health Sci. Eng., 2014, 12 (79), 1.

[12] KITIS M., KAPLAN S., KARAKAYA E., YIGIT O., CIVELEKOGLU G., *Adsorption of natural organic matter from waters by iron coated pumice*, Chemosphere, 2007, 66, 130.

[13] KANG J., LIU H., ZHENG Y.M., QUA J., CHEN J.P., *Systematic study of synergistic and antagonistic effects on adsorption of tetracycline and copper onto a chitosan*, J. Coll. Int. Sci., 2010, 344, 117.

[14] THEVANNAN A., MUNGROO R., HUÍ NÍU C., *Biosorption of nickel with barley straw*, Biores. Techn., 2010, 101, 1776.

[15] LAGERGREN S., *About the theory of so-called adsorption of soluble substances*, Kung. Sven. Veten. Hand., 1898, 1.

[16] HO Y.S., MCKAY G., *Pseudo-second order model for sorption processes*, Proc. Biochem., 1999, 34, 451.

[17] MURUGESAN A., RAVIKUMAR L., SATHYA SELVA BALA V., SENTHIL KUMAR P., VIDHYADEVI T., DINESH KIRUPHA S., KALAIVANI S.S., KRITHIGA S., SIVANESAN S., *Removal of Pb(II), Cu(II) and Cd(II) ions from aqueous solution using polyazomethineamides. Equilibrium and kinetic approach*, Desalination, 2011, 271, 199.

[18] KHATAEE A.R., VAFAEI F., JANNATKHAH M., *Biosorption of three textile dyes from contaminated water by filamentous green algal Spirogyra sp. Kinetic, isotherm and thermodynamic studies*, Int. Biodet. Biodeg., 2013, 83, 33.

[19] HAN R., ZHANG J., ZOU W., SHI J., LIU H., *Equilibrium biosorption isotherm for lead ion on chaff*, J. Hazard Mater., 2005, 125, 266.

[20] CHEN Z., WANG T., JIN X., CHEN Z., MEGHARAJ M., NAIDU R., *Multifunctional kaolinite-supported nanoscale zero-valent iron used for the adsorption and degradation of crystal violet in aqueous solution*, J. Coll. Int. Sci., 2013, 398, 59.

[21] CHEN H., LUOA H., LANA Y., DONG T., HU B., WANG Y., *Removal of tetracycline from aqueous solutions using polyvinylpyrrolidone (PVP-K30) modified nanoscale zero valent iron*, J. Hazard. Mater., 2011, 192, 44.

[22] FANG Z., CHEN J., QIU X., QIU X., CHENG W., ZHU L., *Effective removal of antibiotic metronidazole from water by nanoscale zero-valent iron particles*, Desalination, 2011, 268, 60.

[23] SEPEHR M.N., SIVASANKAR V., ZARRABI M., SENTHIL KUMAR M., *Surface modification of pumice enhancing its fluoride adsorption capacity. An insight into kinetic and thermodynamic studies*, Chem. Eng. J., 2013, 228, 192.

[24] ZHAO Y., GU X., GAO S., GENG J., WANG X., *Adsorption of tetracycline (TC) onto montmorillonite. Cations and humic acid effects*, Geoderma, 2012, 183–184, 12.

[25] HOU M.F., MAC C.X., ZHANG W.D., TANG X.Y., FAN Y.N., WAN H.F., *Removal of Rhodamine B using iron-pillared bentonite*, J. Hazard. Mater., 2011, 186, 1118.
[26] ERSOY B., SARIISIK A., DIKMEN S., SARIISIK G., *Characterization of acidic pumice and determination of its electrokinetic properties in water*, Powder Techn., 2010, 197, 129.
[27] KAPLAN BEKAROĞLU S.S., *Removal of natural organic matter using various surface-modified adsorbents*, Süleyman Demirel University Graduate School of Applied and Natural Sciences, Department of Environmental Engineering, 2010, 284.
[28] CHANG Y., LI C.W., BENJAMIN M.M., *Iron oxide-coated media for NOM sorption and particulate filtration*, J. Amer. Water Works Assoc., 1997, 89, 100.
[29] SMICIKLAS I., DIMOVIC S., PLECAS I., MITRIC M., *Removal of Co^{2+} from aqueous solutions by hydroxyapatite*, Water Res., 2006, 40, 2267.
[30] KHALAF M.A., *Biosorption of reactive dye from textile wastewater by nonviable biomass of Aspergillus niger and Spirogyra sp*., Biores. Techn., 2008, 99, 6631.
[31] ZHAO Y., GENG J., WANG X., GU X., GAO S., *Adsorption of tetracycline onto goethite in the presence of metal cations and humic substances*, J. Coll. Int. Sci., 2011, 361, 247.
[32] ZOLGHARNEIN J., BAGTASH M., SHARIATMANESH T., *Simultaneous removal of binary mixture of Brillant Green and Crystal Violet using derivative spectrophometric determination, multivariate optimization and adsorption characterization of dyes on surfactant modified nano-γ-alumina*, Spectrochim. Acta Part A., Mol. Biomol. Spectry, 2015, 137, 1016.